Probing Erectile Function: *S*-(2-Boronoethyl)-L-Cysteine Binds to Arginase as a Transition State Analogue and Enhances Smooth Muscle Relaxation in Human Penile Corpus Cavernosum[†,‡]

Noel N. Kim,[§] J. David Cox,[||] Ricky F. Baggio,[||] Frances A. Emig,[⊥] Sanjay K. Mistry,[#] Sandy L. Harper,[▽] David W. Speicher,[▽] Sidney M. Morris, Jr.,[#] David E. Ash,[⊥] Abdulmaged Traish,[§] and David W. Christianson*[,||]

Departments of Urology and Biochemistry, Boston University School of Medicine, 700 Albany Street, Boston, Massachusetts 02118, Roy and Diana Vagelos Laboratories, Department of Chemistry, University of Pennsylvania, Philadelphia, Pennsylvania 19104-6323, Department of Biochemistry, Temple University School of Medicine, Philadelphia, Pennsylvania 19140, Department of Molecular Genetics and Biochemistry, University of Pittsburgh School of Medicine, Pittsburgh, Pennsylvania 15261, and the Wistar Institute, 3601 Spruce Street, Philadelphia, Pennsylvania 19104

Received October 3, 2000; Revised Manuscript Received December 21, 2000

ABSTRACT: The boronic acid-based arginine analogue *S*-(2-boronoethyl)-L-cysteine (BEC) has been synthesized and assayed as a slow-binding competitive inhibitor of the binuclear manganese metalloenzyme arginase. Kinetic measurements indicate a K_I value of 0.4−0.6 μM, which is in reasonable agreement with the dissociation constant of 2.22 μM measured by isothermal titration calorimetry. The X-ray crystal structure of the arginase−BEC complex has been determined at 2.3 Å resolution from crystals perfectly twinned by hemihedry. The structure of the complex reveals that the boronic acid moiety undergoes nucleophilic attack by metal-bridging hydroxide ion to yield a tetrahedral boronate anion that bridges the binuclear manganese cluster, thereby mimicking the tetrahedral intermediate (and its flanking transition states) in the arginine hydrolysis reaction. Accordingly, the binding mode of BEC is consistent with the structure-based mechanism proposed for arginase as outlined in Cox et al. [Cox, J. D., Cama, E., Colleluori D. M., Pethe, S., Boucher, J. S., Mansuy, D., Ash, D. E., and Christianson, D. W. (2001) *Biochemistry 40*, 2689−2701.]. Since BEC does not inhibit nitric oxide synthase, BEC serves as a valuable reagent to probe the physiological relationship between arginase and nitric oxide (NO) synthase in regulating the NO-dependent smooth muscle relaxation in human penile corpus cavernosum tissue that is required for erection. Consequently, we demonstrate that arginase is present in human penile corpus cavernosum tissue, and that the arginase inhibitor BEC causes significant enhancement of NO-dependent smooth muscle relaxation in this tissue. Therefore, human penile arginase is a potential target for the treatment of sexual dysfunction in the male.

Approximately, one-half of the male population over the age of 40 suffers from minor, moderate, or severe erectile dysfunction, so this malady presents the broadest and most insidious threat to satisfactory male reproductive health (*1*−*3*). Erectile dysfunction, also referred to as impotence, can result from circulation defects in the smooth muscle vasculature of the corpus cavernosum, a chamber of spongelike tissue that engorges with blood during erection (Figure 1). Defects that compromise cavernosal circulation presumably arise from defects in the highly regulated cascade of enzyme-catalyzed reactions that govern smooth muscle relaxation. Nitric oxide (NO)[1] is a principal regulator of erectile function and mediates nonadrenergic, noncholinergic (NANC) neurotransmission in penile corpus cavernosum smooth muscle, causing rapid relaxation, which in turn leads to erection (*4*−*12*). Therefore, NO synthase is a critical enzyme in smooth muscle physiology.

In smooth muscle tissue, NO synthase is coexpressed with another enzyme of arginine catabolism, arginase, which may play a role in regulating arginine bioavailability to NO synthase (*13*, *14*). Whereas NO synthase catalyzes the oxidation of arginine to form citrulline and NO, arginase catalyzes the hydrolysis of arginine to form ornithine plus urea. On the basis of the consequences of inhibiting arginase activity in NO-producing cells, arginase appears to regulate NO synthase activity—and therefore attenuate NO-dependent physiological processes—by depleting the substrate pool of

[†] This work was supported by grants from the National Institutes of Health: GM49758 (D.W.C.), DK02696 (N.N.K.), DK44841 (D.E.A.), and GM57384 (S.M.M.).

[‡] Atomic coordinates of the complex between arginase and *S*-(2-boronoethyl)-L-cysteine have been deposited in the Research Collaboratory for Structural Bioinformatics with accession code 1HQ5.

* To whom correspondence should be addressed. Phone: (215) 898-5714. Fax: (215) 573-2201. E-mail: chris@xtal.chem.upenn.edu.

[§] Boston University School of Medicine.

[||] University of Pennsylvania.

[⊥] Temple University School of Medicine.

[#] University of Pittsburgh School of Medicine.

[▽] The Wistar Institute.

[1] Abbreviations: ABH, (*S*)-2-amino-6-boronohexanoic acid; BEC, *S*-(2-boronoethyl)-L-cysteine; CHES, 2-(*N*-cyclohexylamino)-ethanesulfonic acid; EFS, electric field stimulation; GAPDH, glyceraldehyde phosphate dehydrogenase; HEPES, *N*-(2-hydroxyethyl)-piperazine-*N*-2-ethanesulfonic acid; NANC, nonadrenergic, noncholinergic; NO, nitric oxide; PSS, physiological salt solution; RT-PCR, reverse transcriptase-polymerase chain reaction.

10.1021/bi002317h CCC: $20.00 © 2001 American Chemical Society
Published on Web 02/02/2001

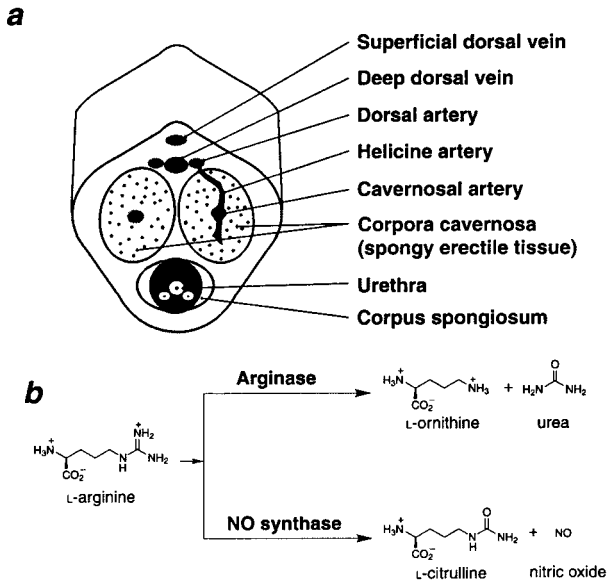

FIGURE 1: (a) Cross-section of the human penis illustrates the anatomy of the corpus cavernosum, a spongy, muscularized tissue that becomes engorged with blood during the erectile process. NO-dependent smooth muscle relaxation in the corpus cavernosum is required for erection. (b) Scheme illustrating the potential regulatory relationship between NO synthase and arginase activities. Arginase activity can potentially deplete the flux of the arginine substrate to NO synthase, which would attenuate NO-dependent smooth muscle relaxation required for penile erection. Therefore, an arginase inhibitor such as BEC could enhance substrate flux to NO synthase, which in turn could enhance NO-dependent smooth muscle relaxation in the corpus cavernosum and thereby enhance penile erection.

arginine that would otherwise be available to NO synthase (Figure 1) (*14*−*18*). Given the recent identification of arginase activity in rabbit and human penile corpus cavernosum tissue (*19*) and the observation that the arginase inhibitor (*S*)-2-amino-6-boronohexanoic acid (ABH) (*20*) facilitates smooth muscle relaxation in rabbit penile corpus cavernosum tissue (*19*), it appears that arginase inhibition indeed enhances NO synthase activity by enhancing the substrate pool of arginine that is available for NO biosynthesis. This conclusion is also supported by detailed studies of ABH-induced gastrointestinal smooth muscle relaxation (*14*).

Arginase requires a spin-coupled $Mn^{2+}-Mn^{2+}$ pair for arginine hydrolysis (*21*−*25*), and the X-ray crystal structure of the arginase trimer reveals that this binuclear manganese cluster resides at the bottom of a ∼15 Å deep active site cleft in each protomer (*26*). Enzymological measurements interpreted in light of the three-dimensional enzyme structure implicate a metal-activated hydroxide mechanism, where the first step of catalysis involves nucleophilic attack of a metal-bridging hydroxide ion at the scissile guanidinium carbon of arginine to form a tetrahedral intermediate, which subsequently collapses to form products ornithine and urea (*26*). The recently determined structure of the arginase−ABH complex provides the first glimpse of transition state binding in the arginase mechanism (*19*). Although, as synthesized, ABH contains a trigonal planar boronic acid that mimics the trigonal planar guanidinium group of the substrate arginine (*20*), this boronic acid moiety undergoes nucleophilic attack by metal-bridging hydroxide ion to yield the tetrahedral boronate anion upon binding to arginase (*19*). Generally speaking, the electron-deficient boron atom of the boronic acid facilitates the addition of a protein-bound or solvent nucleophile to yield a tetrahedral boronate anion that mimics the corresponding tetrahedral intermediate (and the flanking transition states) of a hydrolytic reaction (*27*−*31*).

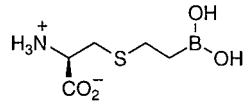

FIGURE 2: Arginase inhibitor *S*-(2-boronoethyl)-L-cysteine (BEC), $K_d = 2.22\ \mu M$.

Here, we report the synthesis and evaluation of the arginine analogue BEC (Figure 2) as a slow-binding inhibitor of arginase. Additionally, we report the X-ray crystal structure of the arginase−BEC complex determined at 2.3 Å resolution from crystals perfectly twinned by hemihedry. This structure reveals that the trigonal planar boronic acid moiety of BEC, like that of ABH (*19*), is attacked by the metal-bridging hydroxide ion upon binding to the active site, thereby yielding the tetrahedral boronate anion. Finally, we demonstrate that BEC does not inhibit NO synthase, and we demonstrate that arginase is expressed in human penile corpus cavernosum. These results set the foundation for physiological studies demonstrating that BEC enhances smooth muscle relaxation in rabbit and human corpus cavernosum tissue, a requirement for penile erection.

MATERIALS AND METHODS

Synthesis of S-(2-Boronoethyl)-L-cysteine (BEC). The hydrochloride salt of BEC was synthesized as described by Matteson, except that the Grignard reagent vinylmagnesium bromide was utilized in the reaction with trimethylborate in the first step of the synthesis (*32*, *33*). All reagents were purchased from Aldrich and used without further purification. Thin-layer chromatography performed on E. Merck silica gel 60 F_{254} glass plates with BEC dissolved in 80:10:10 *n*-butanol:acetic acid:water indicated a single spot with $R_f = 0.44$. ^{1}H NMR (D_2O): δ 0.95 (t, 2H), 2.50 (t, 2H), 2.75−3.05 (m, 2H), 3.72 (m, 1H). ^{11}B NMR (D_2O): δ 31.33 (s). ^{1}H NMR and ^{11}B−NMR spectra were recorded on a Bruker AC-250 (250 MHz) NMR and on a Bruker AC-200 (200 MHz) NMR, respectively; ^{1}H chemical shifts are referenced to HDO and ^{11}B chemical shifts are referenced to BF_3 diethyl ether.

Kinetics of Arginase Inhibition by BEC. Recombinant rat liver arginase was expressed in *Escherichia coli* and purified by modification of the procedure described by Cavalli and colleagues (*34*). Specifically, partially purified protein samples were prepared by chromatography on a Reactive Red-120 dye ligand column (Sigma; 3.3 × 25 cm) instead of the Amicon-Green dye ligand column employed previously (*34*) and eluted with a linear gradient of 0.0 to 0.3 M KCl in 50 mM HEPES−KOH (pH 7.5). The concentrations of enzyme stock solutions were determined by measuring the absorbance at 280 nm using an extinction coefficient of 1.09 mL mg^{-1} cm^{-1} (*35*). Arginase inhibition was evaluated using a modified version of the fixed-point radioactive assay developed by Rüegg and Russell (*36*). Slow onset inhibition was measured by the addition of 0.14 μg of enzyme to assay mixtures containing 100 μM $MnCl_2$, 100 mM CHES−NaOH (pH 9.0), 0.05 μCi L-[guanidino-^{14}C]-arginine (NEN Life Science Products), 10 mM unlabeled L-arginine (approximately 6 × K_M), and varying concentrations of BEC in a

total volume of 1 mL. At the indicated times, 50 μL aliquots were removed and the reactions quenched by the addition of 400 μL of a stop solution containing 0.25 M acetic acid, 7 M urea and a 1:1 v/v slurry of Dowex 50W-X8 at pH 4.5. The resulting mixtures were immediately vortexed, gently mixed for an additional 10 min, and then subject to centrifugation at 6000 rpm for 10 min. Finally, 3 mL of Ecoscint solution (National Diagnostics) was added to 200 μL of supernatant for liquid scintillation counting in a Beckman model LS5000E counter. To study inhibitor release kinetics, the enzyme was incubated with 30 μM BEC in 50 mM HEPES−KOH (pH 7.5) at room temperature. After 10 min, 10 μL of the solution was diluted 100-fold with the standard assay mixture to a final volume of 1 mL, and the production of [^{14}C]urea was monitored as described above. Inhibition constants were determined from the ratio of k_{off}/k_{on} and were also estimated from the final steady-state velocities using the equation for competitive inhibition.

Kinetic assays were also performed using the new chromogenic arginase substrate 1-guanidino-3-nitrobenzene described by Baggio and colleagues (*37*). Reaction velocities were measured at 372 nm, where the liberated chromophore, *m*-nitroaniline, has an extinction coefficient of 1.28×10^3 M^{-1} cm^{-1}. Assays were performed in 100 μM $MnCl_2$, 50 mM bicine-NaOH (pH 9.0), 0.8−2.3 mM 1-guanidino-3-nitrobenzene, and 0.5−9.0 μM BEC. Plots of inverse velocity as a function of inhibitor concentration were nonlinear (data not shown), consistent with the results obtained in the fixed-point radioactive assay.

Isothermal Titration Calorimetry of Arginase−BEC Complexation. All calorimetry experiments were conducted on a MCS isothermal calorimeter from MicroCal, Inc. (Northampton, MA). Arginase was exhaustively dialyzed against 100 μM $MnCl_2$ and 50 mM bicine-NaOH (pH 8.5). Inhibitor was dissolved at a concentration of 1.5 mM in an aliquot of the same buffer. Prior to the titration experiment, samples were degassed under vacuum for 5 min. The sample cell (effective volume 1.366 mL) was overfilled with 1.8 mL of arginase at a concentration of 0.0358 mM and the reference cell was filled with water. The contents of the sample cell were titrated with 30−40 aliquots (2.5 μL each) of inhibitor (an initial 1 μL injection was made, but not used in data analysis). After each injection, the heat change was measured and converted to the corresponding enthalpy value. The reaction mixture was continuously stirred at 400 rpm during titration. Control experiments were carried out by titrating the inhibitor into the buffer solution under identical experimental conditions. Data analysis was performed using Origin software provided with the instrument. The calorimetric data are presented with the background titrations subtracted from the experimental data. The amount of heat produced per injection was calculated by integration of the area under each peak. Data were fit to the equation $q = V\Delta H[E]_t K[L]/(1 + K[L])$, where q is the heat evolved during the course of the reaction, V is the cell volume, ΔH is the binding enthalpy per mole of ligand, $[E]_t$ is the total enzyme concentration, K is the binding constant, and [L] is inhibitor concentration (*38*, *39*).

NO Synthase−BEC Assay. The reagents NADPH, FAD, FMN, L-arginine, HEPES, (6*R*)-5,6,7,8-tetrahydro-L-biopterin (BH_4), and aminoguanidine were purchased from Sigma. Inducible NO synthase was purchased from Alexis Biochemicals and used without further purification. The Nitric Oxide Synthase Colorimetric Assay Kit was purchased from Calbiochem. Materials were used without further purification. The effect of BEC on nitric oxide synthesis was assayed by monitoring the sum of NO_2^- and NO_3^- production (*40*). The enzyme solution of 0.02 mg/mL NO synthase in 50 mM HEPES (pH 7.4), 100 μM NADPH, 4 μM FAD, 4 μM FMN, 6 μM BH_4, 100 μM L-arginine, and 0.0−1.0 mM BEC in a total volume of 100 μL was shaken for 15 min at 37 °C. Reactions were stopped by a 3 min incubation at 100 °C. Nitrate was reduced to nitrite by use of nitrate reductase (40 min at room temperature) and the remaining NADPH was depleted by incubation with lactate dehydrogenase and sodium pyruvate for 20 min at room temperature. Addition of the Griess reagents, sulfanilamide and *N*-(1-naphthyl)-ethylenediamine, converted all available nitrite into a deep purple azo compound; absorbance at 540 nm quantified the extent of NO_x production.

Table 1: Data Collection and Refinement Statistics

resolution (Å)	2.3	solvent atoms (N)[b]	27
total reflections (N)	41 944	manganese ions (N)[b]	2
unique reflections (N)	14 462	R_{twin}[c]	0.158
completeness (%)	98.1	$R_{twin/free}$[c]	0.194
R_{merge}[a]	0.098	Rms deviations	
reflections used in refinement ($>2\sigma$)	14 033	bonds (Å)	0.007
		angles (deg)	1.4
protein atoms (N)[b]	2345	dihedrals (deg)	23.3
inhibitor atoms (N)[b]	13	impropers (deg)	0.9

[a] $R_{merge} = \sum|I_i - \langle I_i\rangle|/\sum|\langle I_i\rangle|$, where I_i is the intensity measurement for reflection i, and $\langle I_i\rangle$ is the mean intensity calculated for reflection i from replicate data. [b] Per monomer. [c] $R_{twin} = \sum||F_{obs}| - [|F_{calc/A}|^2 + |F_{calc/B}|^2]^{1/2}|/\sum|F_{obs}|$, where $|F_{obs}|$ is the observed structure factor amplitude derived from twinned intensity I_{obs}, and $|F_{calc/A}|$ and $|F_{calc/B}|$ are the structure factor amplitudes calculated for the separate twin domains A and B, respectively. R_{twin} underestimates the residual error in the model by averaging the difference between observed and calculated structure factor amplitudes over the two twin-related reflections. The same expression describes $R_{twin/free}$, which was calculated for 1367 test set reflections held aside during refinement.

Crystallization, Data Collection, and Refinement of the Arginase−BEC Complex. Crystals of the arginase−BEC complex were prepared at 4 °C by equilibrating a hanging drop containing 5 μL of protein solution [10 mg/mL arginase, 3 mM BEC, 5 mM $MnCl_2$, and 25 mM bicine-NaOH (pH 8.5)] and 5 μL of precipitant solution [24% poly(ethylene glycol) 1500, 100 mM bicine-NaOH (pH 8.5)] against 1 mL of precipitant solution in the well reservoir. Hexagonal rod-shaped crystals with approximate dimensions $0.1 \times 0.1 \times 0.5$ mm^3 appeared within 4 weeks. Diffraction data to 2.3 Å resolution were collected from a single flash-cooled crystal of the arginase−BEC complex on an R-AXIS IIc image plate detector using a Rigaku RU-200HB rotating anode X-ray generator to provide CuKα radiation at 50 kV/100 mA (λ = 1.5418 Å) (Table 1). Intensity data integration and reduction were performed using DENZO and SCALEPACK, respectively (*41*).

Diffraction intensities exhibited symmetry consistent with space group *P*6 (unit cell parameters $a = b = 91.3$ Å, $c = 69.4$ Å; one monomer in the asymmetric unit), but this assignment was inconsistent with the molecular symmetry of the arginase trimer. Subsequent analysis of measured intensities revealed deviations from Wilson statistics with $\langle I^2\rangle/\langle I\rangle^2 \approx 1.5$ for thin resolution shells, indicative of perfect

hemihedral twinning (*42*) that obscured the true crystallographic symmetry of space group *P*3. Two monomers (from two separate trimers) occupy the asymmetric unit.

For structure determination by the difference Fourier method, initial protein coordinates were those of the complex between arginase and (*S*)-2-amino-6-boronohexanoic acid (ABH) (*19*) less the atoms of the inhibitor and all water molecules. The arginase−ABH complex forms perfectly twinned crystals that are isomorphous with those of the arginase−BEC complex. For calculation of electron density maps, structure factor amplitudes were calculated from deconvoluted intensities using the structure-based algorithm of Redinbo and Yeates (*43*). Initial difference electron density maps calculated for both twin domains with the corresponding deconvoluted structure factor amplitudes revealed that BEC binds to the arginase active site as the tetrahedral boronate anion. Iterative rounds of refinement and rebuilding of the native model were performed using the programs CNS and O, respectively (*44*, *45*). For simultaneous refinement of the arginase−BEC complex in both twin domains against the structure factor amplitudes $|F_{obs}|$ derived from the measured twinned intensities I_{obs}, the target residual was based on the numerator of R_{twin} (Table 1) as implemented in CNS (version 1.0). In the final stages of refinement, the inhibitor BEC was built into the electron density map when R_{twin} decreased to 0.189. Strict noncrystallographic symmetry constraints were initially employed in refinement, and these were ultimately relaxed to appropriately weighted restraints as judged by $R_{twin/free}$. Data collection and refinement statistics are reported in Table 1.

Arginase Expression in Human Penile Corpus Cavernosum. To identify the arginase isoform(s) expressed in human penile corpus cavernosum, reverse transcriptase-polymerase chain reaction (RT-PCR) analysis was performed. Human penile corpus cavernosum tissue was obtained from patients diagnosed with erectile dysfunction of various etiologies who elected to undergo penile prosthesis implantation. These protocols were approved by the Institutional Review Board for Human Studies at the Boston University Medical Center. Cavernosal biopsies were transported to the laboratory in ice-cold physiological salt solution (PSS; 118.3 mM NaCl, 4.7 mM KCl, 0.6 mM $MgSO_4$, 1.2 mM KH_2PO_4, 2.5 mM $CaCl_2$, 25 mM $NaHCO_3$, 0.026 mM $CaNa_2EDTA$, and 11.1 mM glucose). Cavernosal tissue was rinsed to remove blood, cut into strips ($3 \times 3 \times 10$ mm^3), and frozen in liquid nitrogen.

Total RNA was isolated from penile tissue samples using TRIzol reagent (Life Technologies, Inc.). Total RNA from human liver (CLONTECH Laboratories, Inc.) and kidney (Ambion) served as positive controls for expression of arginase I and II, respectively. Five micrograms total RNA was reverse-transcribed in a 20-μL reaction mixture containing 25 ng of oligo dT_{18}, 500 μM deoxynucleoside triphosphates, 10 mM dithiothreitol, 4 μL 5 × RT reaction buffer (Roche Molecular Biochemicals) and 24 units of avian myeloblastosis virus reverse transcriptase (Roche Molecular Biochemicals) at 42 °C for 1 h. Using the conditions listed below, PCR reactions were carried out in a 25-μL reaction mixture containing 80 μM deoxynucleoside triphosphates, 1.5 mM $MgCl_2$, 2.5 μL 10 × PCR reaction buffer (Roche Molecular Biochemicals), 4 pmol of specific primers, cDNA, and 0.8 units of AmpliTaq DNA polymerase (Perkin-Elmer). Amplified products were resolved on a 1% agarose gel containing ethidium bromide. The following PCR primer pairs (synthesized by Life Technologies, Inc.) and conditions were used: arginase I (249 bp product), GTA TAT TGG CTT GAG AGA CG (sense) and GAG ACC TTC TCT GTA TGA CAG [antisense; sequence reported by Haraguchi and colleagues (*46*)], one cycle at 94 °C for 2 min, followed by 25 (liver sample) or 45 cycles (penile samples) at 94 °C for 30 s, 58 °C for 45 s, and 72 °C for 45 s; arginase II (346 bp product), GCG AGT GCA TTC CAT CCT G (sense) and CTA ATG GTA CCG ATT GCC AG [antisense; sequence reported by Morris and colleagues (*47*)], one cycle at 94 °C for 2 min; followed by 25 (kidney sample) or 45 cycles (penile samples) at 94 °C for 30 s, 60 °C for 45 s, and 72 °C for 55 s; glyceraldehyde phosphate dehydrogenase (GAPDH; 184 bp product), ATG ACC ACA GTC CAT GCC ATC ACT (sense) and ACA CGG AAG GCC ATG CCA GTG AG [antisense; sequence reported by Tokunaga and colleagues (*48*)], one cycle at 94 °C for 2 min, followed by 30 cycles at 94 °C for 30 s, 62 °C for 35 s, and 72 °C for 45 s. To clearly distinguish authentic RT-PCR products from PCR products due to possible genomic DNA contamination, each primer in a PCR primer pair was specific for a different exon of the target gene.

Arginase Activity in Human Penile Corpus Cavernosum. Crude tissue extracts were derived from homogenates of human penile corpus cavernosum as previously described (*19*). Arginase enzyme activity in cytosolic extracts of human cavernosal tissue was assessed by the method of Rüegg and Russell (*36*). To determine the inhibitory efficiency of BEC, 10 μL of tissue extract (triplicate aliquots) were incubated in buffer (75 mM glycine, pH 9.0, 0.25 mM $MnCl_2$) containing 300 000 dpm of [^{14}C-guanidino]-L-arginine (51.5 mCi/mmol; NEN Life Science Products, Boston, MA), 2 or 4 mM of unlabeled L-arginine and increasing concentrations of BEC (5−50 μM) in a final volume of 100 μL. Samples were incubated for 60 min at 37 °C and reactions were terminated by the addition of 400 μL of 0.25 M acetic acid (pH 4.5), 7 M urea, 10 mM L-arginine. After the addition of 500 μL of water, samples were passed through a 0.5 mL column of Dowex 50W-X8 resin (Bio-Rad Laboratories, Hercules, CA). Tubes were rinsed twice with 500 μL of water and both rinses were poured onto the columns. Columns were washed with 1 mL of water and all effluent was collected in 20 mL vials. After the addition of 16 mL of Liquiscint (National Diagnostics, Atlanta, GA), radioactivity was quantified by liquid scintillation spectroscopy. Urea production (pmol/min) was normalized to total protein in the tissue extract.

Organ Bath Experiments. All protocols for studies involving human and animal tissues were approved by the Institutional Review Board for Human Studies and the Animal Care and Use Committee at the Boston University Medical Center. Human penile corpus cavernosum tissue was obtained as described in the preceding section and used immediately in organ bath experiments. Rabbit penile corpus cavernosum tissue was obtained from euthanized male New Zealand White rabbits (3.5−4.0 kg body weight), as previously described (*5*). Cavernosal tissue from each rabbit was cut into 4 strips for organ bath experiments.

Human or rabbit cavernosal tissues were mounted onto force transducers (model FT03; Grass Instruments, Quincy,

Scheme 1

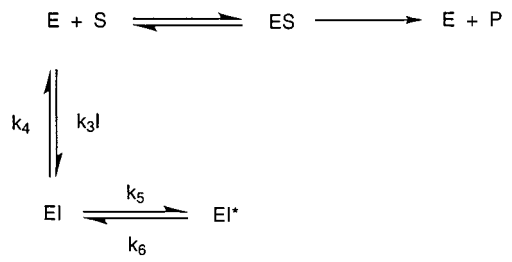

MA) and immersed in 25 mL baths of PSS at 37 °C which were aerated with 5% CO_2, 19% O_2, 76% N_2. All tissues were treated with 3 μM indomethacin, 1 μM atropine, and 10 μM bretylium to inhibit prostanoid production and isolate nonadrenergic, noncholinergic (NANC) responses. Tissue strips were progressively stretched until optimal isometric tension was reached, as described previously (*5*). Cavernosal tissue strips were contracted with 1 μM phenylephrine and subjected to electrical field stimulation (EFS) by means of two platinum plate electrodes, positioned on either side of the tissue, and a current amplifier in series with a square pulse stimulator (model SD9; Grass Instruments, Quincy, MA). Each stimulation period lasted 20 s with trains of square waves having a pulse duration of 0.5 ms and an amplitude of 10 V. Frequency was varied from 0.5 to 15 Hz. All tissues were first subjected to EFS in the absence of arginase inhibitor (vehicle only). Tissues were then incubated with varying concentrations of BEC (0.1−1 mM) for 20 min and electrical stimulations were then repeated. After all stimulations were completed, tissue strips were washed with fresh PSS and treated with 10 μM papaverine and 10 μM nitroprusside to induce maximal relaxation. Changes in tone induced by EFS were expressed as a percentage of maximal relaxation. Responses at each frequency of stimulation, before and after addition of BEC, were compared using paired *t*-test. Comparisons were judged statistically significant if the two-tailed *p*-value was less than or equal to 0.05.

RESULTS

Kinetics and Thermodynamics of Arginase−BEC Complexation. Nonlinearity of kinetic replots in fix-point and continuous arginase assays indicates a complex binding mode for BEC, and slow-onset inhibition is observed in additional fixed-point assays. Typically, slow-binding inhibition is characterized by the initial and rapid formation of a reversible E−I complex, followed by a slow isomerization or conformational change to yield the inhibitory E−I* complex (*49*) (Scheme 1).

Progress curves for the arginase-catalyzed production of urea in the presence of BEC are fit by nonlinear least-squares analysis to the integrated expression

$$P = v_s(t) + (v_o - v_s)(1 - e^{-k}\mathrm{obs}^{(t)})/k_{obs} \qquad (1)$$

where P is the amount of urea formed (in cpm), v_o is the initial rate of urea formation, v_s is the steady-state rate of urea formation, and k_{obs} is the apparent first-order rate constant for the establishment of the equilibrium between EI and EI* (*49*). Progress curves exhibit time-dependent changes in slope, indicative of slow-onset inhibition (Figure 3). Within the limitations of the assay, the initial velocities

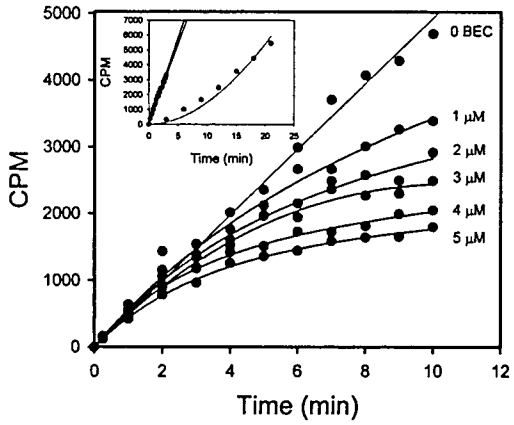

FIGURE 3: Slow-binding inhibition of arginase by BEC. Progress curves are generated as described in Materials and Methods at the indicated concentrations of BEC. The curves represent best fits of the data to eq 1. (Inset) Release of BEC from the arginase−BEC complex. The straight lines correspond to a control assay performed in the absence of BEC and an assay carried out in the presence of 0.3 μM BEC. The curve represents the regain of activity following a 100-fold dilution of the preformed arginase−BEC complex to give a final concentration of 0.3 μM BEC. The data are fit to eq 1.

(v_o) appear to be independent of inhibitor concentration. This raises the possibility that the dissociation constant for the EI complex may be larger than the range of inhibitor concentrations used to generate the progress curves, thereby preventing the observation of the steady-state intermediate EI under initial rate conditions (Scheme 1). Due to these limitations, the binding of inhibitor to the enzyme is assumed to be a single step process with $K_I = k_{off}/k_{on}$:

$$E + I \underset{k_{off}}{\overset{k_{on}}{\rightleftharpoons}} EI^*$$

Accordingly, the association rate constant k_{on} is estimated from a plot of k_{obs} versus [BEC] according to eq 2:

$$k_{obs} = k_{off} + k_{on}[BEC]/(1 + [S]/K_M) \qquad (2)$$

The dissociation rate constant k_{off} is determined by monitoring the rate of return of activity from the enzyme−inhibitor complex through eq 1. Replots of k_{obs} versus [BEC] yield $k_{on} = 1.3 \times 10^3$ M^{-1} s^{-1}. The best fits of inhibitor release data (Figure 3) yield $k_{off} = 4.7 \times 10^{-4}$ s^{-1}. The resultant K_I value of 0.4 μM calculated from these rate constants is in good agreement with the value of 0.6 μM estimated from the steady-state velocities (data not shown).

Importantly, the estimate of arginase−BEC affinity made from kinetic measurements is in reasonable agreement with the direct measurement of the thermodynamic equilibrium constant, $K_d = 2.22$ μM, made by isothermal titration calorimetry (Figure 4). These experiments additionally confirm the expected stoichiometry of inhibitor binding of 0.964/monomer, which indicates essentially complete saturation of arginase active sites by BEC.

BEC Does Not Inhibit NO Synthase. As found for ABH (*19*), BEC does not inhibit NO synthase. Neither 0.1 mM nor 1.0 mM BEC affects NO production (12.4 ± 0.9 and 12.4 ± 1.4 nmol mg^{-1} min^{-1}, respectively) relative to the negative control reaction run in the absence of BEC (13.6 ± 1.3 nmol/mg/min). For reference, inhibition of NO synthase by 10.0 mM aminoguanidine in the positive control

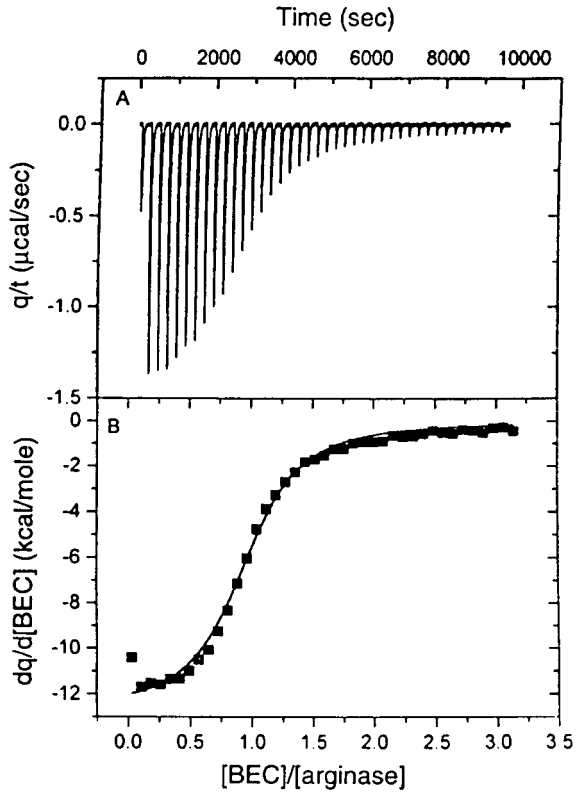

FIGURE 4: Isothermal titration calorimetry of the arginase−BEC complex in 100 μM $MnCl_2$ and 50 mM bicine (pH 8.5) at 25 °C. Shown are the raw data obtained by titration of 0.0358 mM arginase with 40 × 2.5 μL injections of 1.5 mM BEC. The area under each peak is integrated and plotted against [BEC]/[arginase]. The solid line represents the best fit of the experimental data using nonlinear least-squares fitting, indicating (i) a stoichiometry (n) of 0.964 mol of BEC bound/mol of arginase monomer; (ii) an association constant (K_a) of 4.50 × 10^5 M^{-1}, which corresponds to a dissociation constant K_d of 2.22 μM; and (iii) an enthalpy change (ΔH) of −12.75 kcal/mol.

reaction decreases the rate of NO production to 2.4 ± 1.3 nmol mg^{-1} min^{-1}. Therefore, we conclude that BEC is highly selective for inhibition of arginase and not NO synthase. The structural basis for the selectivity of BEC against arginase is that very different transition state structures are required for hydrolysis or oxidation reactions of arginine as catalyzed by arginase and NO synthase, respectively. The boronate anion form of BEC only mimics the transition state for arginine hydrolysis and not that for arginine oxidation.

Structure of the Arginase−BEC Complex. No major tertiary or quaternary structural changes are triggered by inhibitor binding to arginase, and the rms deviation of 308 Cα atoms is 0.35 Å between the native and BEC-complexed arginase monomers. The average thermal *B*-factors of arginase monomers A and B in the asymmetric unit are 23 and 22 $Å^2$, respectively; the average *B*-factors of BEC binding to arginase monomers A and B are 36 and 25 $Å^2$, respectively. The difference in thermal *B*-factors for BEC binding to monomers A and B may arise from slightly different occupancy of inhibitor binding to each monomer in the asymmetric unit of the crystal. An omit map of the arginase−BEC complex shows that the trigonal planar boronic acid group of BEC is bound as the tetrahedral boronate anion, which bridges the binuclear manganese cluster (Figure 5a). The Mn^{2+}_A−Mn^{2+}_B separation increases slightly, from 3.3 Å in the native enzyme (*26*) to 3.4 Å in the enzyme−inhibitor complex, but this difference may be within the experimental error of the crystal structure determination. One boronate hydroxyl group symmetrically bridges the binuclear manganese cluster (O1−Mn^{2+} separations = 2.2 Å) and donates a hydrogen bond to Asp-128, and a second boronate hydroxyl group makes a long coordination interaction with the formerly vacant (*26*) coordination site on Mn^{2+}_A (O2−Mn^{2+}_A separation = 2.5 Å) and donates a hydrogen bond to the backbone C═O of His-141 (O2−O separation = 2.9 Å). Consequently, Mn^{2+}_A undergoes a change in coordination geometry from square pyramidal in the native enzyme (*26*) to distorted octahedral in the enzyme−inhibitor complex; there is no net change in the coordination geometry of Mn^{2+}_B. The third boronate hydroxyl group hydrogen bonds with a water molecule, which in turn hydrogen bonds with the side chain of Thr-246 and a second water molecule. A detailed scheme of enzyme-inhibitor interactions is presented in Figure 5b.

The binding mode of BEC is generally similar to that of ABH (*19*), so the structural basis of the 20-fold affinity difference between the two inhibitors is subtle. The tetrahedral boronate anions of BEC and ABH make identical coordination interactions with the binuclear manganese cluster and hydrogen bond interactions with Asp-128 and the backbone carbonyl of His-141. However, the hydrogen bond interactions of the α-carboxylate and α-amino groups of BEC and ABH have slightly different geometries and bond lengths. These subtle differences appear to arise from geometric differences in the thioester moiety of BEC. In BEC and ABH, the C−S and C−C bond lengths are 1.8 and 1.5 Å, respectively, and the C−S−C and C−C−C bond angles are 97 and 114°, respectively. Given the slightly different molecular geometry for the BEC side chain in comparison with the ABH side chain, and given the resulting subtle differences in enzyme−inhibitor hydrogen bond geometries, it is reasonable that arginase−BEC affinity is slightly compromised in comparison with arginase−ABH affinity.

The binding mode of the tetrahedral boronate anion of BEC, like that of ABH (*19*), mimics the first step of the arginase mechanism proposed upon the completed X-ray crystal structure determination of the native enzyme (*26*). Just as a metal-bridging hydroxide ion is proposed to attack the trigonal planar guanidinium group of the arginine substrate to form the tetrahedral intermediate (Figure 5c), we posit that the metal-bridging hydroxide ion attacks the electrophilic, trigonal planar boronic acid moiety of BEC to form the tetrahedral boronate anion. Accordingly, intermolecular interactions observed in the arginase−BEC complex should correspond to those that contribute to the stabilization of the tetrahedral transition state in arginase catalysis. Both manganese ions of the binuclear manganese cluster play a role in activating the nucleophilic bridging hydroxide ion, and both manganese ions play a role in stabilizing the corresponding hydroxyl group in the tetrahedral intermediate.

The Mn^{2+}_A ion appears to play an additional role beyond the activation of nucleophilic hydroxide ion, and that role is the stabilization of the tetrahedral intermediate and its flanking transition states. As mentioned above, boronate hydroxyl group O2 coordinates to Mn^{2+}_A. By analogy, we predict that the corresponding amino group of the tetrahedral intermediate coordinates to Mn^{2+}_A in arginine hydrolysis as depicted in Figure 5c. This coordination site is vacant in the

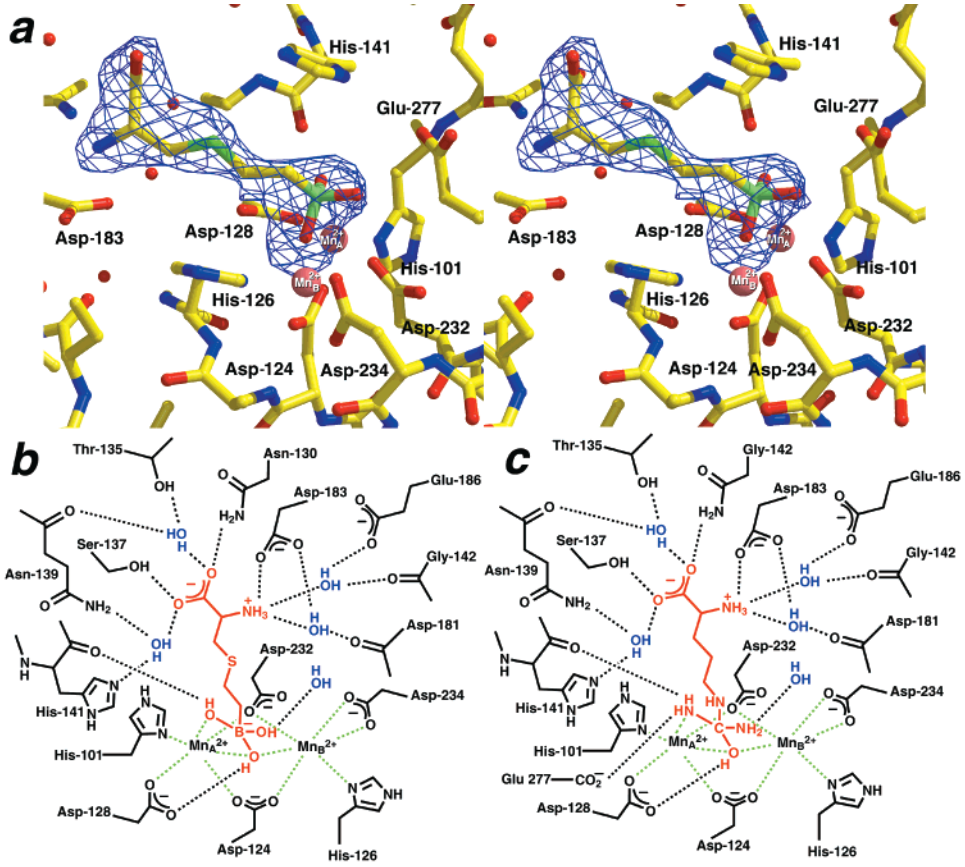

FIGURE 5: (a) Omit electron density map of the arginase−BEC complex calculated with SIGMAA-weighted (78) coefficients $|F_{detwin}| - |F_{calc}|$ averaged over the two monomers in the asymmetric unit. The atoms of BEC were omitted prior to structure-based deconvolution of twinned intensities to minimize model bias in the detwinned structure factor amplitudes $|F_{detwin}|$. The map is contoured at 4σ and selected active site residues are indicated. Atoms are color-coded as follows: C = yellow, O = red, N = blue, S = dark green, B = pale green; water molecules appear as red spheres. Figure generated with BOBSCRIPT (*79*) and Raster3D (*80*). (b) Scheme of arginase−BEC interactions; manganese coordination interactions are indicated by green dashed lines, and hydrogen bonds are indicated by black dashed lines. (c) Stabilization of the tetrahedral intermediate (and flanking transition states) in the arginase mechanism based on the binding mode of BEC. Note that the $Mn^{2+}{}_A$-amino coordination interaction is achieved only as the transition state and tetrahedral intermediate are approached. This coordination interaction is impossible for the substrate prior to catalysis since the corresponding lone electron pair on nitrogen are locked in the guanidinium π system of arginine. Therefore, $Mn^{2+}{}_A$-amino coordination represents a unique mode of transition state stabilization in the arginase mechanism that may partially explain the requirements for two metal ions in catalysis.

native enzyme (*26*), although smeared electron density corresponding to a weakly bound water molecule is observed in one monomer of the native enzyme (*50*). Therefore, the vacant (or readily exchangeable) site on $Mn^{2+}{}_A$ appears to be reserved specifically for coordination by the developing sp^3 lone electron pair on the former guanidino nitrogen as the transition state is approached. Importantly, this lone electron pair is only fully developed when the tetrahedral intermediate is fully formed; prior to nucleophilic attack, the corresponding electron pair on the guanidino nitrogen is delocalized in the "Y"-shaped guanidinium π system and is unavailable for metal coordination:

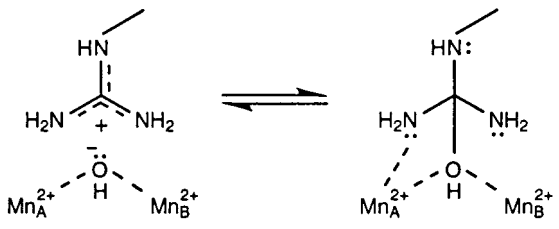

This elegant catalytic strategy underlies the requirement for two manganese ions in catalysis: the second metal ion (i.e., $Mn^{2+}{}_A$) not only assists in the activation of the hydroxide ion nucleophile, but it also stabilizes a chemical functionality unique to the transition state and tetrahedral intermediate in the reaction coordinate of catalysis.

Although it makes van der Waals contacts with BEC hydroxyl groups O2 and O3, Glu-277 does not hydrogen bond with the boronate anion. Modeling experiments indicate that a salt link between Glu-277 and the arginine substrate would orient the scissile guanidinium carbon directly in line for nucleophilic attack by the metal-bridging hydroxide ion (*26*). In support of a precatalytic substrate binding role for Glu-277, subsequent X-ray crystallographic studies of the complex between inactivated arginase from *B. caldovelox* and arginine confirm the salt link between the guanidinium group of arginine and Glu-277 (*51*). Additionally, the structure of the arginase−ornithine−urea ternary complex reveals a hydrogen bond between the urea NH_2 group and Glu-277, thereby implicating Glu-277 in product binding (*52*). That the corresponding hydrogen bond is not observed between the BEC boronate anion and Glu-277 indicates that either (a) electrostatic repulsion between the negatively charged boronate anion and carboxylate group hinders a

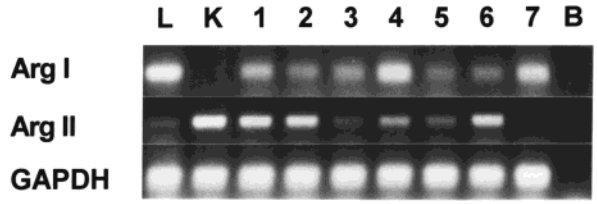

FIGURE 6: Reverse transcriptase-polymerase chain reaction (RT-PCR) analysis of arginase expression in human penile corpus cavernosum. RNA samples from seven individuals have been analyzed by RT-PCR as described in Materials and Methods (lanes 1−7). RNA samples from human liver (lane L) and kidney (lane K) serve as positive controls for arginase I (Arg I) and arginase II (Arg II) mRNAs, respectively. The RT-PCR of GAPDH mRNA confirms mRNA content and integrity of the various samples. The PCR reactions run without added cDNA (lane B) serve as negative controls.

closer interaction or (b) this interaction is important for substrate binding but becomes less important for stabilization of the transition state and tetrahedral intermediate. The structure-based arginase mechanism presented in the accompanying paper by Cox and colleagues (*52*) incorporates the mechanistic insight arising from the structure of the arginase−BEC complex.

Arginase Expression in Human Penile Corpus Cavernosum. Although we have recently measured arginase activity in extracts from rabbit and human penile corpus cavernosum tissue (*19*), we have not confirmed arginase expression in human penile tissue until now. Using RT-PCR analysis, we have identified arginase mRNA in human male corpus cavernosum tissue. Although there appears to be some individual variation in abundance, both arginase I and II mRNAs are clearly detected by RT-PCR analysis of RNA from human penile corpus cavernosum. Analysis of tissue samples from a total of nine individuals diagnosed with erectile dysfunction reveals the presence of arginase I mRNA in eight of the nine samples and arginase II mRNA in all nine samples (results from seven samples are shown in Figure 6). As indicated by the differences in PCR cycle number required for detection (25 cycles for liver and kidney samples versus 45 cycles for penile tissue samples), abundance of arginase mRNAs in human penile tissue is much lower than in human liver or kidney (Figure 6), which are the sites of highest expression of arginases I and II, respectively (*47*, *53*). These results are consistent with the low levels of arginase activity detected in human penile tissue (*19*).

Effect of BEC on Penile Cavernosal Tissue Arginase and Smooth Muscle Contractility. Upon the basis of the activity of BEC against rat liver arginase and the lack of activity against NO synthase, we have tested its efficacy in penile cavernosal tissue extracts by measuring the conversion of [^{14}C]arginine to [^{14}C]urea. In samples of human cavernosal tissue acquired from six men diagnosed with erectile dysfunction, BEC inhibits arginase activity with a mean K_i value of 105.5 ± 22.3 μM as determined by Dixon plot analyses; representative data acquired from one sample are illustrated in Figure 7a. Further studies on smooth muscle function have been performed using organ bath preparations of isolated cavernosal tissue strips. Electrical stimulation of tissue strips treated with an adrenergic nerve blocker (bretylium) and a muscarinic receptor antagonist (atropine) elicits frequency-dependent, neurogenic relaxation responses, which are primarily mediated by nitric oxide (*4*−*7*). Nitric oxide-

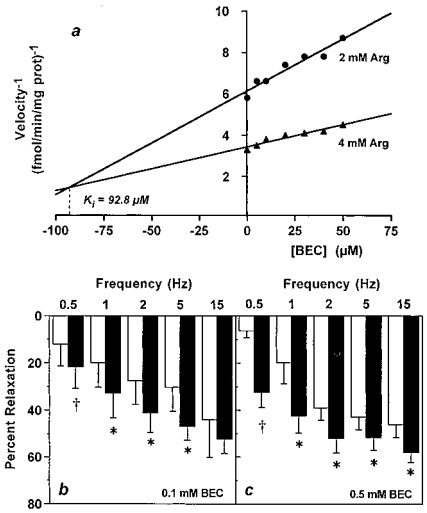

FIGURE 7: Effect of BEC in human penile corpus cavernosum tissue. (a) Arginase activity in the presence of increasing concentrations of BEC is assessed at two different concentrations of substrate. Shown is a representative Dixon plot for tissue acquired from one of six human patients diagnosed with erectile dysfunction; the mean K_i value for six different tissue samples is 105.5 ± 22.3 μM. (b, c) Effects of BEC on smooth muscle function are assessed in organ bath preparations of human cavernosal tissues. The NANC relaxation responses are elicited by electric field stimulation in the presence of vehicle (white bars). Tissues were then treated with varying concentrations of BEC for 20 min and electric stimulations were repeated (black bars). Data are expressed as mean ± SEM [(*) $p \leq 0.05$; (†) $p \leq 0.005$].

mediated relaxation is significantly enhanced by BEC in both human and rabbit tissues (Figure 7, panels b and c, and Table 2). On average, the largest enhancement is 5.1-fold in human tissue at 0.5 mM BEC and 3.3-fold in rabbit tissues at 1 mM BEC. Interestingly, the highest concentration of BEC (1 mM) is the most effective at potentiating neurogenic relaxation in rabbit tissue, whereas responses were not further enhanced by concentrations greater than 0.5 mM BEC in human tissue.

DISCUSSION

Structural Aspects of BEC Binding and the Arginase Mechanism. The boronic acid moiety is suitable for incorporation into a reaction coordinate analogue due to the electron-deficient nature of boron (*27*−*31*), which facilitates nucleophilic attack of a solvent molecule to generate the boronate anion. Indeed, the neutral trigonal planar boronic acid exists in solution in a pH-dependent equilibrium with the tetrahedral boronate anion: at alkaline pH values, i.e., high (HO^-), the tetrahedral boronate anion predominates. For example, 1-butane boronic acid is >99% trigonal planar boronic acid at pH 8.0, and the hydration reaction $RB(OH)_2 + H_2O \Leftrightarrow RB(OH)_3^- + H^+$ has pK_a = 10.6 (*54*). Since the crystal structure of the arginase−BEC complex conclusively reveals that the tetrahedral BEC boronate anion binds to arginase, the boronic acid hydration reaction contributes to the observed dissociation constant for the enzyme−inhibitor complex.

Strictly speaking, boronic acid inhibitors of hydrolytic enzymes cannot be classified as chemically inert, preformed transition state analogues, since a discrete chemical step—the boronic acid hydration reaction—is required to convert

Table 2: Effect of BEC on Non-Adrenergic, Non-Cholinergic Relaxation Responses in Rabbit and Human Penile Corpus Cavernosum

		percent relaxation				
treatment	*N*	0.5 Hz	1 Hz	2 Hz	5 Hz	15 Hz
human						
vehicle	5	12.0 ± 9.3	19.9 ± 10.4	27.5 ± 10.1	30.2 ± 10.1	43.9 ± 16.0
0.1 mM BEC	5	21.6 ± 9.2[b]	32.6 ± 10.5[c]	40.9 ± 8.4[c]	46.8 ± 5.9[c]	52.2 ± 6.1
vehicle	6	6.3 ± 2.9	19.9 ± 8.9	38.9 ± 5.3	42.8 ± 5.4	45.9 ± 5.4
0.5 mM BEC	6	32.3 ± 6.4[b]	42.2 ± 7.3[c]	51.8 ± 6.3[c]	51.5 ± 5.4[c]	57.9 ± 4.3[c]
vehicle	3	14.3 ± 11.0	16.3 ± 12.7	36.5 ± 10.4	37.3 ± 14.1	35.9 ± 8.0
1.0 mM BEC	3	23.1 ± 9.9[c]	34.7 ± 9.5	37.74 ± 11.4	35.1 ± 11.7	40.1 ± 13.3
rabbit						
vehicle	4	19.4 ± 6.4	42.7 ± 8.7	59.1 ± 7.2	70.6 ± 6.2	79.1 ± 3.5
0.1 mM BEC	4	42.4 ± 7.9	60.7 ± 4.7	73.9 ± 4.2[c]	81.2 ± 2.6	87.7 ± 4.6
vehicle	4	23.8 ± 6.4	52.1 ± 14.8	64.1 ± 16.5	70.7 ± 13.6	78.5 ± 10.2
0.5 mM BEC	4	46.0 ± 13.5[c]	64.3 ± 18.2	74.2 ± 15.9	77.9 ± 14.4	82.8 ± 9.2
vehicle	4	7.08 ± 1.64	20.5 ± 4.5	36.1 ± 6.4	51.3 ± 6.1	62.9 ± 6.5
1.0 mM BEC	4	23.8 ± 3.3[c]	36.4 ± 6.2[c]	62.3 ± 4.6[c]	68.9 ± 2.0[c]	79.2 ± 6.5

[a] Isolated tissue strips were treated with bretylium and atropine, contracted with 1 μM phenylephrine and subjected to electrical stimulation in the presence of vehicle. Tissue strips were treated for 20 min with BEC and electrical stimulations were repeated. All data are expressed as mean ± SEM. [b] $p \leq 0.005$. [c] $p \leq 0.05$, compared to vehicle at same frequency of stimulation.

the inhibitor into a species that more closely resembles the transition state. Instead, boronic acid inhibitors such as BEC can be considered chemically reactive substrate analogues that can be reversibly converted into transition state analogues upon binding to a target enzyme. Such inhibitors have been informally designated as "reaction coordinate analogues" (*55*), since the discrete chemical step required for tight-binding inhibition precisely mimics a chemical step leading to the transition state(s) along the reaction coordinate of hydrolysis. In the example of arginase−BEC association, the tighter-binding form of BEC is one that resembles the tetrahedral intermediate [which by Hammond's Postulate (*56*) is energetically and structurally similar to its flanking transition states]. Thus, the preferential binding of BEC as the tetrahedral boronate anion directly reflects Pauling's observation that an enzyme preferentially binds the transition state (or a corresponding analogue), rather than the substrate or product (*57*, *58*). We conclude that the tetrahedral boronate anion form of BEC is a faithful analogue of the tetrahedral intermediate and its flanking transition states in arginase catalysis, and the observed intermolecular interactions summarized in Figure 5b stabilize the actual tetrahedral intermediate and its flanking transition states in arginase catalysis as depicted in Figure 5c.

Given the slow-binding kinetics measured for arginase−BEC complexation (Figure 3), it is tempting to speculate that the slow EI → EI* conversion (Scheme 1) corresponds to the nucleophilic attack of metal-bridging hydroxide ion at the trigonal planar boronic acid. Studies with microsomal and cytosolic leucine aminopeptidases (which are both binuclear metallohydrolases) and α-aminoboronic acid inhibitors similarly reveal slow-binding inhibition kinetics, and detailed analysis suggests that the slow-binding step represents the formation of the tetrahedral boronate anion from the trigonal planar boronic acid substrate analogue (*31*). Moreover, the binding of 1-butaneboronic acid to the binuclear zinc aminopeptidase from *Aeromonas proteolytica* reveals that the boronic acid moiety is trapped in an arrested form between the Michaelis complex and the transition state for hydration in the enzyme active site (*59*). Despite the analogous implication that the trigonal planar form of BEC initially binds to arginase and subsequently undergoes nucleophilic attack by metal-bridging hydroxide ion, we cannot conclusively rule out that the preformed tetrahedral boronate anion form of BEC directly displaces metal-bridging hydroxide ion to yield the inhibitory complex observed in the crystal structure.

Arginase in Erectile Physiology. The selectivity of BEC toward arginase and the lack of activity against NO synthase allow us to probe the role of arginase in the regulation of human corpus cavernosum smooth muscle tone. The detection of mRNA for arginase types I and II in this tissue (Figure 6) further supports our detection of arginase activity in human corpus cavernosum tissue extracts (*19*) (Figure 7a). Interestingly, BEC exhibits a significantly higher K_i value against the arginase activity measured in tissue extracts than against the activity of purified enzyme preparations. This difference may be rationalized by the presence of endogenous arginine in tissue preparations and also the potential interactions of BEC with other cellular constituents. Notably, however, the related inhibitor ABH exhibits virtually identical K_i values of ∼0.1 μM against the arginase activities of gastrointestinal smooth muscle extracts and purified enzyme preparations (*16*, *37*), so differences between in vitro and ex vivo measurements with BEC may arise from other factors. For example, it is conceivable that oxidation of the BEC thioester results in a sulfoxide or sulfone derivative with attenuated arginase affinity and biological activity, and that such oxidation is facilitated in tissue extracts. Regardless, the functional enhancement of neurogenic relaxation in penile cavernosal tissue exposed to BEC (Figure 7), as well as comparable levels of enhancement achieved with ABH treatment (*19*), supports a role for arginase in regulating NO biosynthesis. This interaction between arginase and NO synthase may become particularly important in disease states resulting from neuropathies, endothelial dysfunction and/or compromised smooth muscle responsiveness. This is suggested by our observation that BEC causes a greater degree of enhancement in human tissue derived from men with erectile dysfunction, relative to "healthy" rabbit tissue.

Previous reports by other investigators document the influence of arginase on inducible NO synthase (*15*−*18*); however, these situations only arise during conditions of sepsis, in which an abnormally high demand is made on

available arginine stores by inducible NO synthase and a consequent overproduction of NO. To date, the only examples of nonpathological regulation of NO production by arginase are in gastrointestinal smooth muscle tissue (*14*) and genito-urinary smooth muscle tissue (*19*). It remains to be seen whether other tissues containing arginase and NO synthase exhibit such a mechanism of regulation or whether gastrointestinal and genito-urinary tissues are unique in this regard. While it is presumed that arginase is co-localized with NO synthase in the nerves and endothelial cells of cavernosal tissue, its distribution has yet to be confirmed. By way of comparison, a recent study suggests that arginase and NO synthase may be localized in different but neighboring cells (*60*). Future studies investigating the cellular distribution of arginase and correlating these findings with NO synthase distribution patterns in penile erectile tissue will aid in the distinction between intercellular and intracellular mechanisms of regulation.

The Arginine Paradox. That BEC enhances NANC nerve-mediated smooth muscle relaxation is consistent with the proposal that arginase regulates arginine bioavailability for NO biosynthesis and NO-dependent relaxation of human corpus cavernosum smooth muscle. However, that arginine bioavailability appears to limit NO biosynthesis is somewhat surprising, since intracellular arginine concentrations of 100−800 μM (*61*, *62*) greatly exceed the K_M value of 1 μM measured for endothelial NO synthase (*63*). At such substrate concentrations, the rate of NO biosynthesis ought to exceed 99% maximal velocity, so modest increases in arginine concentrations should have essentially no effect on increasing NO production. Nevertheless, NO production is indeed enhanced by elevated extracellular arginine concentrations despite such high intracellular concentrations, and this phenomenon embodies the paradox (*62*).

This paradox may be resolved by complex cellular trafficking schemes for arginine that, to date, are only partly delineated. Since intracellular arginine concentrations can be varied over a wide range without affecting NO biosynthesis (*64*), it appears that intracellular pools of arginine are compartmentalized within the cell and sequestered away from NO synthase; moreover, these intracellular pools are not fully exchangeable with extracellular arginine (*65*). The notion of discrete intracellular arginine pools is further supported by the finding that overexpression of arginase in endothelial cells significantly reduces NO production despite the fact that intracellular arginine concentrations remain greater than 1.6 mM (*66*). Given that NO biosynthesis is sensitive to extracellular arginine concentrations (*67*−*69*), it appears that extracellular arginine—but not intracellular arginine—is preferentially delivered to NO synthase, possibly by association with the plasma membrane cationic amino acid transporters (*70*−*72*). The apparent K_M values of 68 μM and 100 μM for extracellular arginine uptake by cultured endothelial cells (*72*) and neurons (*73*), respectively, are close to the K_M values of 100−150 μM measured for arginine transport systems (*74*). An additional factor in the cellular compartmentalization and trafficking of arginine is the presence and compartmentalization of endogenous competitive inhibitors, such as N^G-methyl-L-arginine and N^G,N^G-dimethyl-L-arginine, that would elevate the effective K_M for arginine with endothelial NO synthase (*65*). Such inhibitors would have to be displaced from the NO synthase active site by the substrate, which would require higher effective concentrations of arginine.

Since the arginase inhibitors ABH and BEC enhance NO-dependent smooth muscle relaxation (Figure 7) (*14*, *19*), and since ABH and BEC are highly selective toward arginase inhibition due to the specific boronic acid hydration chemistry required to convert these reaction coordinate analogues into tight-binding inhibitors (Figure 5) (*19*), arginase is strongly implicated in the modulation of arginine pools that are delivered to neuronal and endothelial NO synthase. Whether arginase can modulate the trafficking of arginine to NO synthase localized in neurons and in the Golgi and caveolae of endothelial cells (*75*, *76*), remains a critical question to be addressed in future studies.

Concluding Remarks. The results of these interdisciplinary studies in structural biology, chemistry, and physiology confirm the presence and activity of arginase in human corpus cavernosum tissue. Moreover, the arginase inhibitor BEC enhances the NO-dependent relaxation of human corpus cavernosum smooth muscle, which implicates arginase as a regulator of arginine bioavailability to NO synthase. Therefore, we conclude that human penile arginase is a potential target for the treatment of sexual dysfunction in the male. The localization of NO synthase in human clitoral corpus cavernosum may similarly implicate arginase as a regulator of arginine bioavailability in this tissue (*77*), so we speculate that arginase may likewise be a potential target for the treatment of sexual dysfunction in the female.

ACKNOWLEDGMENT

We thank Evis Cama for many helpful discussions.

REFERENCES

1. Kinsey, A. C., Pomeroy, W. B., and Martin, C. E., Eds. (1948) *Sexual Behavior in the Human Male*, W. B. Saunders, Philadelphia.
2. NIH Consensus Development Panel on Impotence (1993) *J. Am. Med. Assoc. 270*, 83−90.
3. Feldman, H. A., Goldstein, I., Hatzichristou, D. G., Krane, R. J., and McKinlay, J. B. (1994) *J. Urol. 151*, 54−61.
4. Ignarro, L. J., Bush, P. A., Buga, G. M., Wood, K. S., Fukuto, J. M., and Rajfer, J. (1990) *Biochem. Biophys. Res. Commun. 170*, 843−850.
5. Kim, N., Azadzoi, K., Goldstein, I., and Saenz de Tejada, I. (1991) *J. Clin. Invest. 88*, 112−118.
6. Burnett, A. L., Lowenstein, C. J., Bredt, D. S., Chang, T. S., and Snyder, S. H. (1992) *Science 257*, 401−403.
7. Rajfer, J., Aronson, W. J., Bush, P. A., Dorey, F. J., and Ignarro, L. J. (1992) *New Engl. J. Med. 326*, 90−94.
8. Burnett, A. L., Tillman, S. L., Chang, T. S., Epstein, J. I., Lowenstein, C. J., Bredt, D. S., and Snyder, S. H. (1993) *J. Urol. 150*, 73−76.
9. Lugg, J. A., Gonzalez-Cadavid, N. F., and Rajfer, J. (1995) *J. Androl. 16*, 2−4.
10. Burnett, A. L., Ricker, D. D., Chamness, S. L., Maguire, M. P., Crone, J. K., Bredt, D. S., Snyder, S. H., and Chang, T. S. (1995) *Biol. Reprod. 52*, 1−7.
11. Burnett, A. L., Nelson, R. J., Calvin, D. C., Liu, J. X., Demas, G. E., Klein, S. L., Kriegsfeld, L. J., Dawson, V. L., Dawson, T. M., and Snyder, S. H. (1996) *Mol. Med. 2*, 288−296.
12. Burnett, A. L. (1997) *J. Urol. 157*, 320−324.
13. Wei, L. H., Jacobs, A. T., Morris, S. M., Jr., and Ignarro, L. J. (2000) *Am. J. Physiol. 279*, C248−C256.
14. Baggio, R., Emig, F. A., Christianson, D. W., Ash, D. E., Chakder, S., and Rattan, S. (1999) *J. Pharmacol. Exp. Ther. 290*, 1409−1416.

15. Hey, C., Boucher, J.-L., Vadon-Le Goff, S., Ketterer, G., Wessler, I., and Racke, K. (1997) *Br. J. Pharmacol. 121*, 395−400.
16. Chang, C. I., Liao, J. C., and Kuo, L. (1998) *Am. J. Physiol. 274*, H342−H348.
17. Tenu, J.-P., Lepoivre, M., Moali, C., Brollo, M., Mansuy, D., and Boucher, J.-L. (1999) *NO Biol. Chem. 3*, 427−438.
18. Morris, S. M., Jr. (1999) in *Cellular and Molecular Biology of Nitric Oxide* (Laskin, J. D., and Laskin, D. L., Eds.) pp 57−85, New York, Marcel Dekker, Inc.
19. Cox, J. D., Kim, N. N., Traish, A. M., Christianson, D. W. (1999) *Nat. Struct. Biol. 6*, 1043−1047.
20. Baggio, R., Elbaum, D., Kanyo, Z. F., Carroll, P. J., Cavalli, R. C., Ash, D. E., and Christianson, D. W. (1997) *J. Am. Chem. Soc. 119*, 8107−8108.
21. Herzfeld, A., and Raper, S. M. (1976) *Biochem. J. 153*, 469−478.
22. Reczkowski, R. S., and Ash, D. E. (1992) *J. Am. Chem. Soc. 114*, 10992−10994.
23. Reczkowski, R. S., and Ash, D. E. (1994) *Arch. Biochem. Biophys. 312*, 31−37.
24. Christianson, D. W. (1997) *Prog. Biophys. Mol. Biol. 67*, 217−252.
25. Ash, D. E., Cox, J. D., and Christianson, D. W. (2000) Manganese and Its Role in Biological Processes. In *Metal Ions in Biological Systems* (Sigel, A., and Sigel, H., Eds.) Vol. 37, pp 407−428, Marcel Dekker, New York.
26. Kanyo, Z. F., Scolnick, L. R., Ash, D. E., and Christianson, D. W. (1996) *Nature 383*, 554−557.
27. Koehler, K. A., and Leinhard, G. E. (1971) *Biochemistry 10*, 2477−2483.
28. Philipp, M., and Bender, M. L. (1971) *Proc. Natl. Acad. Sci. U.S.A. 68*, 478−480.
29. Baker, J. O., Wilkes, S. H., Bayliss, M. E., and Prescott, J. M. (1983) *Biochemistry 22*, 2098−2103.
30. Kettner, C. A., and Shenvi, A. B. (1984) *J. Biol. Chem. 259*, 15106−15114.
31. Shenvi, A. B. (1986) *Biochemistry 25*, 1286−1291.
32. Matteson, D. S., Soloway, A. H., Tomlinson, D. W., Campbell, J. D., and Nixon, G. A. (1964) *J. Med Chem. 7*, 640−643.
33. Matteson, D. S. (1960) *J. Am. Chem. Soc. 82*, 4228−4233.
34. Cavalli, R. C., Burke, C. J., Kawamoto, S., Soprano, D. R., and Ash, D. E. (1994) *Biochemistry 33*, 10652−10657.
35. Schimke, R. T. (1970) *Methods Enzymol. 17a*, 313−317.
36. Rüegg, U. T., and Russell, A. S. (1980) *Anal. Biochem. 102*, 206−212.
37. Baggio, R., Cox, J. D., Harper, S. L., Speicher, D. W., and Christianson, D. W. (1999) *Anal. Biochem. 276*, 251−253.
38. Fisher, H. F., and Singh, N. (1995) *Methods Enzymol. 259*, 194−221.
39. Wiseman, T., Williston, S., Brandts, J. F., and Lin, L.-N. (1989) *Anal. Biochem. 179*, 131−137.
40. Verdon, C. P., Burton, B. A., and Prior, R. L. (1995) *Anal. Biochem. 224*, 502−508.
41. Otwinowski, Z., and Minor, W. (1997) *Methods Enzymol. 276*, 307−326.
42. Yeates, T. O. (1997) *Methods Enzymol. 276*, 344−358.
43. Redinbo, M. R., and Yeates, T. O. (1993) *Acta Crystallogr., Sect. D 49*, 375−380.
44. Brünger, A. T., Adams, P. D., Clore, G. M., DeLano, W. L., Gros, P., Grosse-Kunstleve, R. W., Jiang, J. S., Kuszewski, J., Nilges, M., Pannu, N. S., Read, R. J., Rice, L. M., Simonson, T., and Warren, G. L. (1998) *Acta Crystallogr., Sect. D 54*, 905−921.
45. Jones, T. A., Zou, J.-Y., Cowan, S. W., and Kjeldgaard, M. (1991) *Acta Crystallogr., Sect. A 47*, 110−119.
46. Haraguchi, Y., Takiguchi, M., Amaya, Y., Kawamoto, S., Matsuda, I., and Mori, M. (1987) *Proc. Natl. Acad. Sci. U.S.A. 84*, 2412−2415.
47. Morris, S. M., Jr., Bhamidipati, D., and Kepka-Lenhart, D. (1997) *Gene 193*, 157−161.
48. Tokunaga, K., Nakamura, Y., Sakata, K., Fujimori, K., Ohkubo, M., Sawada, K., and Sakiyama, S. (1987) *Cancer Res. 47*, 5616−5619.
49. Morrison, J. F., and Walsh, C. T. (1988) *Adv. Enzymol. 61*, 201−301.
50. Kanyo, Z. F. (1996) Ph.D. Dissertation, University of Pennsylvania.
51. Bewley, M. C., Jeffrey, P. D., Patchett, M. L., Kanyo, Z. F., and Baker, E. N. (1999) *Structure 7*, 435−448.
52. Cox, J. D., Cama, E., Colleluori, D. M., Pethe, S., Boucher, J. L., Mansuy, D., Ash, D. E., and Christianson, D. W. (2001) *Biochemistry 40*, 2689−2701.
53. Vockley, J. G., Jenkinson, C. P., Shukla, H., Kern, R. M., Grody, W. W., and Cederbaum, S. D. (1996) *Genomics 38*, 118−123.
54. Baker, J. O., and Prescott, J. M. (1983) *Biochemistry 22*, 5322−5331.
55. Christianson, D. W., and Lipscomb, W. N. (1989) *Acc. Chem. Res. 22*, 62−69.
56. Hammond, G. S. (1955) *J. Am. Chem. Soc. 77*, 334−338.
57. Pauling, L. (1948) *Nature 161*, 707−709.
58. Wolfenden, R. (1976) *Annu. Rev. Biophys. Bioeng. 5*, 271−306.
59. De Paola, C. C., Bennett, B., Holz, R. C., Ringe, D., and Petsko, G. A. (1999) *Biochemistry 38*, 9048−9053.
60. Braissant, O., Gotoh, T., Loup, M., Mori, M., and Bachmann, C. (1999) *Mol. Brain Res. 70*, 231−241.
61. Wu, G., and Morris, S. M., Jr. (1998) *Biochem. J. 336*, 1−17.
62. Förstermann, U., Closs, E. I., Pollock, J. S., Nakane, M., Schwarz, P., Gath, I., and Kleinert, H. (1994) *Hypertension 23*, 1121−1131.
63. Griffith, O. W., and Stuehr, D. J. (1995) *Annu. Rev. Physiol. 57*, 707−736.
64. Arnal, J.-F., Münzel, T., Venema, R. C., James, N. L., Bai, C.-I., Mitch, W. E., and Harrison, D. G. (1995) *J. Clin. Invest. 95*, 2565−2572.
65. Leiper, J., and Vallance, P. (1999) *Cardiovasc. Res. 43*, 542−548.
66. Li, H., Meininger, C. J., Hawker, J. R., Jr., Haynes, T. E., Kepka-Lenhart, D., Mistry, S. K., Morris, S. M., Jr., and Wu, G. (2001) *Am. J. Physiol. 280*, E75−E82.
67. Aisaka, K., Gross, S. S., Griffith, O. W., and Levi, R. (1989) *Biochem. Biophys. Res. Commun. 163*, 710−717.
68. Cooke, J. P., Andon, N. A., Girerd, X. J., Hirsch, A. T., and Creager, M. A. (1991) *Circulation 83*, 1057−1062.
69. Eddahibi, S., Adnot, S., Carville, C., Blouquit, Y., and Raffestin, B. (1992) *Am. J. Physiol. 263*, L194−L200.
70. McDonald, K. K., Rouhani, R., Handlogten, M. E., Block, E. R., Griffith, O. W., Allison, R. D., and Kilberg, M. S. (1997) *Biochim. Biophys. Acta 1324*, 133−141.
71. McDonald, K. K., Zharikov, S., Block, E. R., and Kilberg, M. S. (1997) *J. Biol. Chem. 272*, 31213−31216.
72. Closs, E. I., Scheld, J.-S., Sharafi, M., and Förstermann, U. (2000) *Mol. Pharmacol. 57*, 68−74.
73. Westergaard, N., Beart, P. M., and Schousboe, A. (1993) *J. Neurochem. 61*, 364−367.
74. Closs, E. I. (1996) *Amino Acids 11*, 193−208.
75. Sessa, W. C., Garcia-Cardena, G., Liu, J., Keh, A., Pollock, J. S., Bradley, J., Thiru, S., Braverman, I. M., and Desai, K. M. (1995) *J. Biol. Chem. 270*, 17641−17644.
76. Liu, J., Garcia-Cardena, G., and Sessa, W. C. (1996) *Biochemistry 35*, 13277−13281.
77. Burnett, A. L., Calvin, D. C., Silver, R. I., Peppas, D. S., and Docimo, S. G. (1997) *J. Urol. 158*, 75−78.
78. Read, R. J. (1986) *Acta Crystallogr., Sect. A 42*, 140−149.
79. Esnouf, R. M. (1997) *J. Mol. Graphics 15*, 132−134.
80. Merritt, E. A., and Bacon, D. J. (1997) *Methods Enzymol. 277*, 505−524.

BI002317H